UC Berkeley
UC Berkeley Previously Published Works

Title

Synthesis of Pt3Y and Other Early–Late Intermetallic Nanoparticles by Way of a Molten Reducing Agent

Permalink

https://escholarship.org/uc/item/79x7h4fw

Journal

Journal of the American Chemical Society, 139(16)

ISSN

0002-7863

Authors

Kanady, Jacob S
Leidinger, Peter
Haas, Andreas
et al.

Publication Date

2017-04-26

DOI

10.1021/jacs.7b01366

Peer reviewed

Synthesis of Pt$_3$Y and other Early-Late Intermetallic Nanoparticles by way of a Molten Reducing Agent

Jacob S. Kanady[†+], Peter Leidinger[§], Andreas Haas[§], Sven Titlbach[*], Stephan Schunk[*], Kerstin Schierle-Arndt[+], Ethan J. Crumlin,[x] Cheng Hao Wu,[‡] A. Paul Alivisatos[†‡∥⊥*]

[†]Department of Chemistry, University of California—Berkeley, Berkeley, California 94720, USA

[+]California Research Alliance by BASF, University of California, Berkeley, California 94720, United States

[§]BASF SE, 67056 Ludwigshafen am Rhein, Germany

[*]hte GmbH – a subsidiary of BASF, 69123 Heidelberg, Germany

[x]Advanced Light Source, Lawrence Berkeley National Laboratory, Berkeley, California 94720, United States

[‡]Materials Sciences Division, Lawrence Berkeley National Laboratory, Berkeley, California 94720, United States

[∥]Kavli Energy NanoScience Institute, Berkeley, California 94720, United States

[⊥]Department of Materials Science and Engineering, University of California, Berkeley, California 94720, United States

Supporting Information Placeholder

ABSTRACT: Early-late intermetallic phases have garnered increased attention recently for their catalytic properties. To achieve the high surface areas needed for industrially relevant applications, these phases must be synthesized as nanoparticles in a scalable fashion. Herein, Pt$_3$Y—targeted as a prototypical example of an early-late intermetallic—has been synthesized as nanoparticles approximately 5-20 nm in diameter in a solution process and characterized by XRD, TEM, EDS and XPS. The key development is the use of a molten borohydride (MEt$_3$BH, M= Na, K) as both the reducing agent and reaction medium. Readily available halide precursors of each metal are used. Accordingly, no organic ligands/surfactants are necessary as the resulting halide salt byproduct prevents sintering, which further permits dispersion of the nanoscale intermetallic onto a support. The versatility of this approach was validated by synthesis of other intermetallic phases such as Pt$_3$Sc, Pt$_3$Lu, Pt$_2$Na and Au$_2$Y.
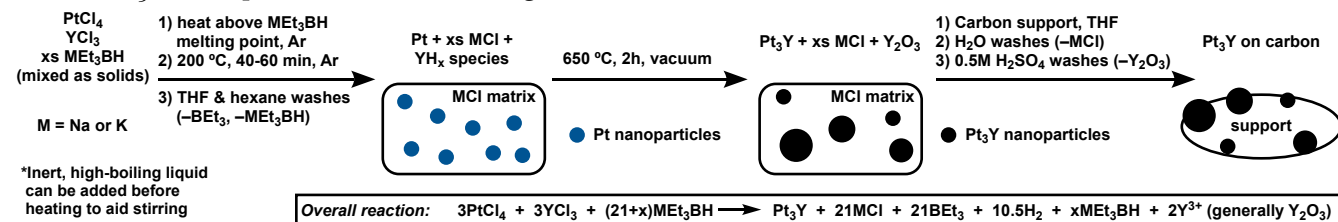
The late transition metals readily alloy with elements that have much more negative reduction potentials such as the alkaline, alkaline earth, and rare earth metals and form a range of intermetallic (IM) phases.[1] Recently, a number of papers have predicted—and experimental work confirmed—that some of these early-late intermetallic phases have exceptional catalytic activity and/or stability. Nørskov and coworkers predicted that Pt$_3$Y would be more active than pure Pt in the oxygen reduction reaction based on computations of the oxygen adsorption energy for a Pt overlayer on the intermetallic.[2] Indeed, bulk polycrystalline electrodes of Pt$_3$Y were 6-10 times more active than pure Pt at 0.9-0.87 V vs. RHE.[2] Other Pt IM phases such as Pt$_5$Tb, Pt$_5$Gd, and Pt$_5$Ca have been shown to be high quality oxygen reduction catalysts as well.[3] Outside of catalysis, IMs of the alkali metals with Au have been predicted to be good candidates for plasmonic applications.[4]

Exploration of the potential applications of these materials would be greatly facilitated by a scalable synthesis of the IM phases in the nanoparticulate form. Pt/Y IM nanoparticles have been synthesized, but only by two low-throughput, μg-scale physical means: a co-sputter technique,[5] and a gas aggregation technique.[6] Other reports of Pt/Y nanoparticles synthesized by chemical means do not have firm evidence of a Pt$_n$Y IM phase.[7]

A chemical, solution phase synthesis of early metal intermetallics is difficult due to the early metals' extreme oxygen affinity and very negative reduction potentials: ca. −2.37 V for Y^{3+}/Y as opposed to +1.2V for Pt^{2+}/Pt. Indeed, a recent review described it as "almost impossible."[8] The strict absence of oxygen and water—or any protic solvent, making the well-

studied polyol process[9] unworkable—is an absolute necessity, and only the strongest reducing agents can work. For example, *n*BuLi can be added to Au nanoparticles to form Au_3Li,[10] and KEt_3BH is strong enough to reduce $TiCl_4$ with $PtCl_4$ together in THF to form Pt_3Ti nanoparticles after annealing.[11] Anoth-er challenge is the high temperature sometimes needed to achieve the structural ordering of an IM phase rather than simply an alloy, the IM often being crucial to catalytic activity.[11-12] This rules out organic surfactants during the annealing step, as they will

Scheme 1. Process scheme for the synthesis of Pt_3Y nanoparticles.

decompose and potentially contaminate the nano-particle surfaces. Salt[13] and oxide[14] matrices have been used to great effect to prevent sintering and control particle size during annealing steps.

We initially targeted alkali metal triethylborohy-drides as strong reducing agents for their ability to reduce early metal halides such as $TiCl_3$ or $TiCl_4$ in THF[15] and its success for other Pd and Pt IM phases.[11, 13, 16] In our hands, YCl_3 could not be reduced with KEt_3BH at room temperature in THF, and if $PtCl_4$ was included in the reaction, only pure Pt was observed. This is consistent with literature: an Y^{3+} complex with two Et_3BH^- anions coordinated has been characterized.[17] In searching for more extreme reducing conditions, we noted that the melting points of the solvent-free triethylborohydrides are quite low: 30° and 95 °C for the Na and K salts, respectively. Although only commercially available as solutions in THF or toluene, they can be isolated as white, crystalline powders if handled carefully.[18] Therefore, we hypothesized that a molten triethyl-borohydride salt could be the extremely reducing environment that could afford yttrium reduction. Moreover, as long as halide salts of platinum and yttrium were used, the byproduct NaX or KX salts would stabilize the newly formed Pt/Y nanoparticles to sintering and growth.

Mixing $PtCl_4$, YCl_3, and KEt_3BH as solids at room temperature affords no reaction: the orange color of $PtCl_4$ does not change. However, heating the mixture past the melting point of the KEt_3BH turns the mixture black, consistent with metal nanoparticle formation. The molten salt solution is then heated to 200 °C for 30-60 minutes to ensure completion. After cooling, liquid BEt_3 is observed above a black precipitate. The excess borohydride and byproduct borane are washed away with thoroughly dried THF and hexane under strictly air and water-free conditions. The resulting grey or black powder is sealed in a quartz tube under vacuum and annealed at 650 °C for 2 hours. The resulting Pt_3Y nanoparticles are released from the salt matrix by washing with water in the presence of a carbon support, affording supported Pt_3Y nanoparticles. Any Y_2O_3 formed from the excess YCl_3 is removed with acid. (Scheme 1; See Supporting Information for experimental details).

TEM images of the particles show their size between 5-20 nm, with some larger agglomerates (Figure 1). Collection of EDS spectra on multiple areas of the TEM grid confirm a Pt/Y ratio of 3:1 (Figure S1). High-resolution images show lattice spacing of ~2.35 Å, more
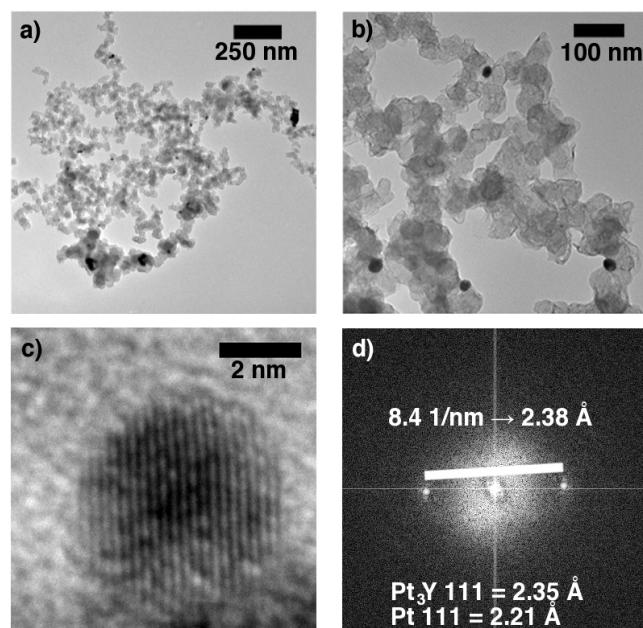

Figure 1. TEM images of Pt_3Y nanoparticles dispersed onto a carbon support (a & b). c) HRTEM image of a Pt_3Y nanoparticle (scale bar = 2 nm) and its corresponding FFT image (d). The lattice spacing in (c) matches the 111 reflection of Pt_3Y.

consistent with Pt$_3$Y (111 at 2.35 Å) than Pt (111 at 2.27 Å) (Figure 1c,d). The polydispersity observed is consistent with other salt stabilized IM particles that with only a small excess of salt, larger, polydisperse particles were observed.[13] Based on the stoichiometry of our system—21 KCl formed per Pt$_3$Y—some polydispersity is therefore expected.

Crystalline, intermetallic Pt$_3$Y was also confirmed by powder XRD (Figure 2). The XRD pattern could be indexed left-shifted from the pure Pt reference indicating an expansion of the unit cell of pure metallic Pt stemming from the higher atomic radii of Y (180 ppm) compared to Pt (135 ppm). In detail, the 111 reflection is observed at 44° 2θ—compared to 46.5° 2θ for pure Pt (Figure 2; Co X-ray source, WL = 1.79 Å). Most tellingly, the presence of the *100, 110, 210, 211, 221,* and *310* reflections confirms formation of the ordered intermetallic Pt$_3$Y phase in the cubic Cu$_3$Au structure type (*Pm-3m* space group) rather than a disordered alloy. One should note that the observed diffraction patterns are shifted from those found in the databases for Pt$_3$Y, representing a ca. 1% increase in the unit cell edge from
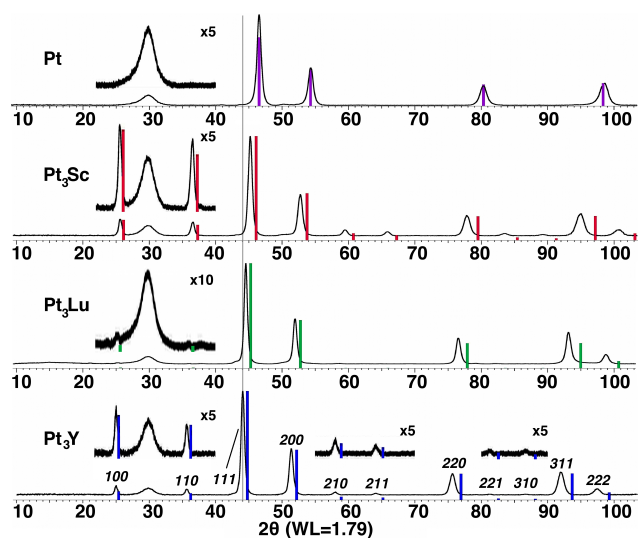

Figure 2. pXRD of Pt$_3$M & Pt nanoparticles synthesized in molten NaEt$_3$BH & KEt$_3$BH, respectively. The blue, green, red and purple lines represent database patterns for Pt$_3$Y (PDF 03-065-5161), Pt$_3$Lu (PDF 03-065-5757), Pt$_3$Sc (PDF 03-065-8049) and Pt (PDF 00-004-0802). The grey line is a guide to show the smaller Pt$_3$Lu, Pt$_3$Sc, and Pt unit cells as compared to Pt$_3$Y. The insets emphasize the presence of reflections for the ordered IM *Pm-3m* Pt$_3$M phases and their absence for Pt. The peak at 30° is from the CRC-III carbon support. The X-ray wavelength is 1.79 Å (Co Kα).

a = 4.069(3) Å (PDF 03-065-5161) to a = 4.126(2) Å. Others have observed similar unit cell expansions in IM nanoparticles. Sun *et al.* observed a unit cell

expansion in PtFe nanoparticles after annealing at 750 °C to form the face-centered tetragonal IM phase[14]—citing nanoparticle surface effects and imperfect phase formation—as did Peter *et al.* in their synthesis of Pd$_2$Ge—citing Ge deficiency.[16] Another possible explanation is a small amount of interstitial hydride: as the reducing agent is a hydride donor, platinum and yttrium hydride intermediates are likely and residual hydride may be present even after annealing. Similar unit cell expansions have been observed in the nickel-metal-hydride literature for substoichiometric interstitial hydride.[19]

XPS characterization[20] confirms the presence of Y°. A low photon energy of 350 eV—190 eV kinetic energy for the Y 3d region—probes 0.6 nm into the surface[21] and shows Y$_2$O$_3$ at 158.5 eV and 160.5 eV with a small Y° peak at 155.8 eV (Figure 3a). A higher photon energy of 760 eV (600 eV kinetic energy) probes 1 nm into the surface and the Y° signal becomes more pronounced (Figure 3b). This depth profiling suggests oxidation of Y° from the surface layers and retention of Y° below ca. 1 nm, as has been seen in the literature for bulk Pt/Y IM.[12] Both photon energies show pure Pt° (Figure S2). These observations are consistent with EDS mapping of the Pt$_x$Y nanoparticles synthesized by gas aggregation, which showed a Pt overlayer of ~1 nm over the IM phase containing the Y°.[6a]
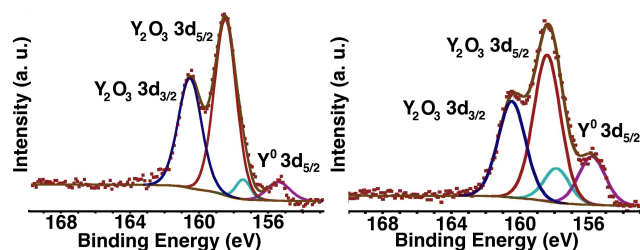

Figure 3. XPS spectra of Pt$_3$Y nanoparticles dropcast onto a gold substrate focused on the Y 3*d* region. Photon energies of 350 eV (a) and 760 eV (b) were used and referenced to the Au 4$f_{7/2}$ peak (84.0 eV) at each respective photon energy. See the SI for fitting parameters.

Once convinced that Pt$_3$Y was successfully formed, optimization of the process was undertaken. Initially, a large excess of borohydride was used—ca. 4-5x excess—for the practical reason that stirring was poor without enough molten salt. Much of the excess (now only 1.5x needed) could be replaced with a small amount of an, inert high boiling liquid such as dioctyl ether, 1,3-diisopropylbenzene, or trioctylamine. This helped stirring and afforded a cleaner product (Figure S3). NaEt$_3$BH was also

found to work well; notably, in control experiments without YCl₃, Pt₂Na was observed with NaEt₃BH, while only Pt° was observed with KEt₃BH, consistent with Pt/K alloy formation being thermodynamically disfavored (Figure S4).[1]

TEM and XRD characterization pre- and post-anneal gives some insight into the mechanism of the reaction. After heating to 200 ºC and washing with THF/hexanes, but before the 650 ºC anneal, the NaCl or KCl is the only visible phase, with very broad Pt° visible in some cases (Figure S5). No crystalline yttrium-containing phases are visible, suggesting that they either remain amorphous or are already incorporated into the Pt as a disordered alloy. It is clear that the yttrium does react in some way, for if it remained as YCl₃ it would be washed away with the THF. As proposed for the Pt₃Ti and Pt₃V syntheses in the literature,[11] an yttrium hydride intermediate is likely. TEM shows small <4 nm particles in the salt matrix, consistent with the very broadened XRD pattern (Figure S6). After annealing to 650 ºC under vacuum, Pt₃Y, KCl or NaCl, and Y₂O₃ are observed by XRD (Figure S5). It is not clear how the excess yttrium in the reaction is converted to the oxide; possibly trace oxygen impurities are introduced during the tube sealing process. Also of note in Figure S6 is the clear broadening of the Pt₃Y peak relative to the sharp KCl peaks; Scherer analysis gives crystalline domains ca. 10-15 nm in diameter, consistent with TEM, which shows the particles dispersed in the salt matrix (Figure S6). The Pt₃Y pattern broadening is kept through the acid washes.

Pt₃Sc and Pt₃Lu have also been synthesized with this process, affording similar particle sizes (Figure S7) and correspondingly smaller unit cells as observed by XRD (Figure 2). Like Pt₃Y, these phases are also shifted relative to the database values, consistent with ~1% elongation of the unit cell edge (Table S1). EDS confirms the presence of Sc and Lu after acid washes (Figure S8 & S9). If PtCl₄ is replaced with AuCl₃, Au₂Y is observed with a Au₂Na impurity (Figure S10).

In conclusion, the trialkylborohydride molten salt has proven itself as a highly reducing reaction medium, affording the first chemical synthesis of the Pt₃Y intermetallic phase in nanoparticulate form. The nanoparticles are 5-20 nanometers in diameter, with some larger agglomerates, and the process can be generalized to other difficult early-late IM phases. Incorporation of additional salt matrix to help control particle size is a crucial, further point for improvement, as is leaching of the particles from the salt and stabilization as a colloidal suspension by organic ligands/surfactants for further processing. We predict this method will be applicable to not only other difficult-to-reduce metals and metal combinations, but also other chemistries that need a polar, harshly reducing environment as supplied by the trialkylborohydride molten salt. Increasing the scale and optimization of the particle/support system and incorporation into electrochemical and gas-phase reactors is ongoing for future catalyst applications.

ASSOCIATED CONTENT

Supporting Information. The Supporting Information is available free of charge on the ACS Publications website.

Procedures for nanoparticle formation and support incorporation; further TEM, XRD, EDX and XPS analysis. (PDF)

AUTHOR INFORMATION

Corresponding Author

*alivis@berkeley.edu
Notes
The authors declare no competing financial interest.

ACKNOWLEDGMENT

REFERENCES

1. de Boer, F. R.; Boom, R.; Mattens, W. C. M.; Miedema, A. R.; Niessen, A. K., *Cohesion in Metals: Transition Metal Alloys*. North-Holland Physics Publishing: New York, U.S., 1988.

2. Greeley, J.; Stephens, I. E. L.; Bondarenko, A. S.; Johansson, T. P.; Hansen, H. A.; Jaramillo, T. F.; Rossmeisl, J.; Chorkendorff, I.; Norskov, J. K., *Nat. Chem.* 2009, 1, 552-556.

3. (a) Escudero-Escribano, M.; Verdaguer-Casadevall, A.; Malacrida, P.; Gronbjerg, U.; Knudsen, B. P.; Jepsen, A. K.; Rossmeisl, J.; Stephens, I. E. L.; Chorkendorff, I., *J. Am. Chem. Soc.* 2012, 134, 16476-16479; (b) Malacrida, P.; Escudero-Escribano, M.; Verdaguer-Casadevall, A.; Stephens, I. E. L.; Chorkendorff, I., *J. Mater. Chem. A* 2014, 2, 4234-4243; (c) Escudero-Escribano, M.; Malacrida, P.; Hansen, M. H.; Vej-Hansen, U. G.; Velazquez-Palenzuela, A.; Tripkovic, V.; Schiotz, J.; Rossmeisl, J.; Stephens, I. E. L.; Chorkendorff, I., *Science* 2016, 352, 73-76.

4. (a) Blaber, M. G.; Arnold, M. D.; Ford, M. J., *J. Phys.-Condens. Mat.* **2010,** *22*; (b) Cortie, M. B.; McDonagh, A. M., *Chem. Rev.* **2011,** *111*, 3713-3735.

5. (a) Hwang, S. J.; Kim, S. K.; Lee, J. G.; Lee, S. C.; Jang, J. H.; Kim, P.; Lim, T. H.; Sung, Y. E.; Yoo, S. J., *J. Am. Chem. Soc.* **2012,** *134*, 19508-19511; (b) Yoo, S. J.; Lee, K. S.; Hwang, S. J.; Cho, Y. H.; Kim, S. K.; Yun, J. W.; Sung, Y. E.; Lim, T. H., *Int. J. Hydrogen Energ.* **2012,** *37*, 9758-9765.

6. (a) Hernandez-Fernandez, P.; Masini, F.; McCarthy, D. N.; Strebel, C. E.; Friebel, D.; Deiana, D.; Malacrida, P.; Nierhoff, A.; Bodin, A.; Wise, A. M.; Nielson, J. H.; Hansen, T. W.; Nilsson, A.; Stephens, I. E. L.; Chorkendorff, I., *Nat. Chem.* **2014,** *6*, 732-738; (b) Velazquez-Palenzuela, A.; Masini, F.; Pedersen, A. F.; Escudero-Escribano, M.; Deiana, D.; Malacrida, P.; Hansen, T. W.; Friebel, D.; Nilsson, A.; Stephens, I. E. L.; Chorkendorff, I., *J. Catal.* **2015,** *328*, 297-307.

7. (a) Jeon, M. K.; McGinn, P. J., *J. Power Sources* **2011,** *196*, 1127-1131; (b) Nishanth, K. G.; Sridhar, P.; Pitchumani, S., *Electrochem. Commun.* **2011,** *13*, 1465-1468; (c) Seo, M. H.; Choi, S. M.; Seo, J. K.; Noh, S. H.; Kim, W. B.; Han, B., *Appl. Catal. B-Environ.* **2013,** *129*, 163-171; (d) Han, S. B.; Kwak, D. H.; Lee, Y. W.; Kim, S. J.; Lee, J. Y.; Lee, S.; Kwon, H. J.; Park, K. W., *Int. J. Electrochem. Sci.* **2016,** *11*, 3803-3814; (e) Brandiele, R.; Durante, C.; Gradzka, E.; Rizzi, G. A.; Zheng, J.; Badocco, D.; Centomo, P.; Pastore, P.; Granozzi, G.; Gennaro, A., *J. Mater. Chem. A* **2016,** *4*, 12232-12240.

8. Furukawa, S.; Komatsu, T., *ACS Catal.* **2017,** *7*, 735-765.

9. (a) Cable, R. E.; Schaak, R. E., *Chem. Mater.* **2005,** *17*, 6835-6841; (b) Schaak, R. E.; Sra, A. K.; Leonard, B. M.; Cable, R. E.; Bauer, J. C.; Han, Y. F.; Means, J.; Teizer, W.; Vasquez, Y.; Funck, E. S., *J. Am. Chem. Soc.* **2005,** *127*, 3506-3515.

10. Bondi, J. F.; Schaak, R. E., *Eur. J. Inorg. Chem.* **2011,** 3877-3880.

11. Cui, Z.; Chen, H.; Zhao, M. T.; Marshall, D.; Yu, Y. C.; Abruna, H.; DiSalvo, F. J., *J. Am. Chem. Soc.* **2014,** *136*, 10206-10209.

12. Stephens, I. E. L.; Bondarenko, A. S.; Bech, L.; Chorkendorff, I., *Chemcatchem* **2012,** *4*, 341-349.

13. Chen, H.; Wang, D. L.; Yu, Y. C.; Newton, K. A.; Muller, D. A.; Abruna, H.; DiSalvo, F. J., *J. Am. Chem. Soc.* **2012,** *134*, 18453-18459.

14. Kim, J. M.; Rong, C. B.; Liu, J. P.; Sun, S. H., *Adv. Mater.* **2009,** *21*, 906-909.

15. Bonnemann, H.; Brijoux, W.; Brinkmann, R.; Fretzen, R.; Joussen, T.; Koppler, R.; Korall, B.; Neiteler, P.; Richter, J., *J. Mol. Catal.* **1994,** *86*, 129-177.

16. Sarkar, S.; Jana, R.; Suchitra; Waghmare, U. V.; Kuppan, B.; Sampath, S.; Peter, S. C., *Chem. Mater.* **2015,** *27*, 7459-7467.

17. Lyubov, D. M.; Fukin, G. K.; Trifonov, A. A., *Inorg. Chem.* **2007,** *46*, 11450-11456.

18. Binger, P.; Benedikt, G.; Rotermun.Gw; Koster, R., *Liebigs Ann. Chem.* **1968,** *717*, 21-40.

19. (a) Lynch, J. F.; Reilly, J. J., *J Less-Common Met* **1982,** *87*, 225-236; (b) Karonik, V. V.; Tsypin, M. I.; Prokofev, M. V.; Kazakov, D. N., *Zh. Neorg. Khim.* **1983,** *28*, 191-194.

20. Grass, M. E.; Karlsson, P. G.; Aksoy, F.; Lundqvist, M.; Wannberg, B.; Mun, B. S.; Hussain, Z.; Liu, Z., *Rev. Sci. Instrum.* **2010,** *81*, 053106.

21. Powell, C. J.; Jablonski, A., *NIST Electron Inelastic-Mean-Free-Path Database Version 1.1.* National Institute of Standards and Technology: Gaithersburg, MD, 2000.

Insert Table of Contents artwork here